Author(s): Nau, Werner M.; Moorthy, Suresh; Lambert, Hugues; Mohan, Neetha; Schwarzlose, Thomas; Kalenius, Elina; Lee, Tung-Chun

Title: Noncovalent Modulation of Chemoselectivity in the Gas Phase Leads to a Switchover in Reaction Type from Heterolytic to Homolytic to Electrocyclic Cleavage

Year: 2023

Version: Published version

How to cite: *Angew. Chem. Int. Ed.* **2023**, *62*, e202303491
doi.org/10.1002/anie.202303491

Host-Guest Systems

Noncovalent Modulation of Chemoselectivity in the Gas Phase Leads to a Switchover in Reaction Type from Heterolytic to Homolytic to Electrocyclic Cleavage

Suresh Moorthy[+], Hugues Lambert[+], Neetha Mohan, Thomas Schwarzlose, Werner M. Nau, Elina Kalenius,* and Tung-Chun Lee**

Abstract: In the gas phase, thermal activation of supramolecular assemblies such as host–guest complexes leads commonly to noncovalent dissociation into the individual components. Chemical reactions, for example of encapsulated guest molecules, are only found in exceptional cases. As observed by mass spectrometry, when 1-amino-methyl-2,3-diazabicyclo[2.2.2]oct-2-ene (DBOA) is complexed by the macrocycle β-cyclodextrin, its protonated complex undergoes collision-induced dissociation into its components, the conventional reaction pathway. Inside the macrocyclic cavity of cucurbit-[7]uril (CB7), a competitive chemical reaction of monoprotonated DBOA takes place upon thermal activation, namely a stepwise homolytic covalent bond cleavage with the elimination of N_2, while the doubly protonated CB7·DBOA complex undergoes an inner-phase elimination of ethylene, a concerted, electrocyclic ring-opening reaction. These chemical reaction pathways stand in contrast to the gas-phase chemistry of uncomplexed monoprotonated DBOA, for which an elimination of NH_3 predominates upon collision-induced activation, as a heterolytic bond cleavage reaction. The combined results, which can be rationalized in terms of organic-chemical reaction mechanisms and density-function theoretical calculations, demonstrate that chemical reactions in the gas phase can be steered chemoselectively through noncovalent interactions.

Introduction

Chemists have developed numerous tools to control chemical reactivity in the condensed phase, prominently through variations of the solvent and microenvironment.[1–4] In the gas phase, the situation is considerably more challenging, with mode-selective chemistry having emerged as an elegant approach, in which individual bonds can be selectively vibrationally excited by laser irradiation, leading in the ideal case to a preferential bond cleavage.[5–7] An alternative approach to modulate chemical reactivity in the gas phase is through noncovalent interactions, for example through the formation of host–guest complexes.[8–12] Previously, we have demonstrated that covalent bond cleavage in a supramolecular complex can become favored over its noncovalent dissociation and that certain chemical reactions can be effectively suppressed by macrocyclic encapsulation.[13] In detail, for a series of bicyclic azoalkanes, host–guest dissociation, which generally prevails upon thermal excitation of noncovalent complexes in the gas phase, could be suppressed in favor of an electrocyclic cleavage of the guest, namely a retro-Diels–Alder reaction, taking place inside the macrocyclic cavity. This observation has opened a new playground to explore how chemical reactivity can be directed in the gas phase through noncovalent interactions, which we are now entering.

Specifically, we have pursued the possibility to not only suppress certain reactions but to switch on new reaction pathways, to control the cleavage of certain bonds over those of others and, thereby, to mimic the aim of mode-selective chemistry through a supramolecular approach. Our efforts have led us to a showcase where not only different covalent reactions can be affected in the inner phase of a macrocycle, but where the entire spectrum of organic-

[*] Dr. S. Moorthy,[+] Dr. H. Lambert,[+] Dr. N. Mohan, Dr. T.-C. Lee
Institute for Materials Discovery, University College London (UCL)
London WC1H 0AJ (UK)
E-mail: tungchun.lee@ucl.ac.uk

Dr. H. Lambert,[+] Dr. T.-C. Lee
Department of Chemistry, University College London (UCL)
London WC1H 0AJ (UK)

T. Schwarzlose, Prof. W. M. Nau
School of Science, Constructor University
28759 Bremen (Germany)
E-mail: wnau@constructor.university

Dr. E. Kalenius
Department of Chemistry, University of Jyväskylä
Jyväskylä (Finland)
E-mail: elina.o.kalenius@jyu.fi

[+] These authors contributed equally to this work.

chemical reaction types (heterolytic, homolytic, and electrocyclic bond cleavage) can be covered.

In detail, building on the observation that bicyclic azoalkanes can undergo concomitant chemical reactions inside macrocycles, we investigated functionalized derivatives with competitive covalent reaction pathways. When screening different candidates (Figure S1), we identified 1-amino-methyl-2,3-diazabicyclo[2.2.2]oct-2-ene (DBOA) as promising model system with multimodal chemical reactivity (Figure 1). As size-matching hosts, cucurbit[7]uril (CB7) and β-cyclodextrin (β-CD) were chosen.

Results and Discussion

Stoichiometric (1:1) complexes of β-CD or CB7 with DBOA are spontaneously formed by self-assembly in aqueous media. The complexes are of the inclusion type (*endo*), which can be demonstrated by several techniques, conventionally by ^{1}H NMR. The host–guest complexation is driven by a combination of electrostatic interactions and hydrophobic effects, resulting in host-characteristic aqueous binding constants of $K_a = 250\ M^{-1}$ for β-CD and $K_a = 2.2 \times 10^{10}\ M^{-1}$ for CB7.[14,15] Both (protonated) supramolecular complexes could be transferred in their intact form to the gas phase by using electrospray ionization in a mass spectrometer under ultrahigh vacuum conditions (see Supporting Information Section 1 for experimental details). The chemical reactivity of the encapsulated DBOA was investigated by using collision-induced dissociation (CID)[13] of the isolated ions of interest. CID is an ergodic process which allows energy randomization such that scission of the weakest bond is expected. For noncovalent host–guest complexes the "weakest link" is the noncovalent one, because intermolecular (supramolecular) interactions are typically 1–2 orders of magnitude weaker than covalent or ionic chemical bonds. Accordingly, CID of host–guest complexes results generally in the dissociation of the complex, that is, the formation of the isolated intact host and guest.[16–19] However, the complexes of bicyclic azoalkanes with CB7 have been found to be a notable violation this rule,[13] which we have now exploited to unveil an exciting gas-phase chemistry.

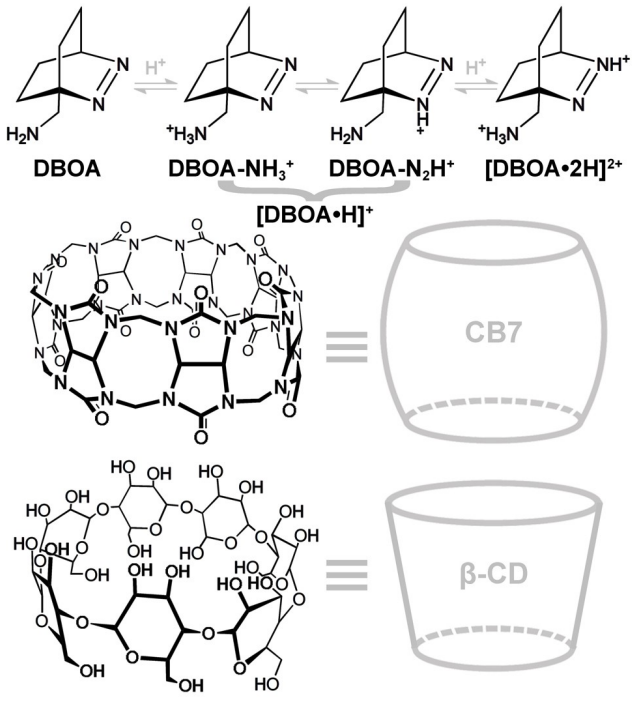

Figure 1. Chemical structures of the amino-functionalized bicyclic azoalkane DBOA (in different protonation states) as a guest as well as of the macrocyclic hosts cucurbit[7]uril (CB7) and β-cyclodextrin (β-CD).

Qualitative insights into the reaction pathways can be obtained by analyzing the CID data of DBOA and its complex with the macrocyclic hosts (Figure 2). In the absence of a macrocycle, an aqueous solution of DBOA affords $[DBOA{\cdot}H]^+$ as base peak in its mass spectrum, no doubly protonated ions were observed even in the presence of strong acid (Figure S2). CID experiments establish the elimination of NH_3 as the major reaction pathway (ca. 90 %), while the elimination of C_2H_4 (ca. 10 %) is observed as a minor route (Figure 2a,e & Figure S4). The elimination of NH_3 requires the amino group to be protonated ($DBOA\text{-}NH_3^+$ in Figure 1) to allow for a heterolytic cleavage mechanism. Computational methods (Supporting Information Section 5) predict the protonation of the azo group to be energetically favorable in the gas phase (Figure 3a), contrary to the intuitively expected aqueous pK_a-based situation, but a fast shuttling of the proton between the neighboring nitrogen atoms becomes feasible through a quasi-hydrogen bonded geometry (Figure 3a). Vice versa, protonation of the azo group facilitates a retro-Diels–Alder reaction,[20] which leads to an electrocyclic elimination of C_2H_4 as a minor reaction pathway of uncomplexed $[DBOA{\cdot}H]^+$.

The CID effects of the host–guest complexes varied in dependence on the macrocycle. For the $[\beta\text{-}CD{\cdot}DBOA{\cdot}H]^+$ complex, only dissociation of the supramolecular complex into its components, $[DBOA{\cdot}H]^+$ and β-CD, was observed. This corresponds to a noncovalent bond dissociation, the standard pathway for dissociation of host–guest complexes (Figure 2d,h). A different result was expected for CB7 as macrocycle, because it is known for its constrictive binding.[13] Indeed, CID of the $[CB7{\cdot}DBOA{\cdot}H]^+$ complex afforded not only host–guest dissociation, but also chemical reactions of the guest under formation of host-*product* complexes. Surprisingly, while two bond cleavage pathways with two different reaction types (heterolytic vs electrocyclic) were found to be immanent for uncomplexed $[DBOA{\cdot}H]^+$, both routes are shut down upon CB7 inclusion complex formation. Instead, when the host–guest complex $[CB7{\cdot}DBOA{\cdot}H]^+$ is thermally activated under CID conditions, it eliminates N_2 (Figure 2b,f). Although the fragments C_2H_4 and N_2 are isobaric and have the same nominal mass (28 u), the latter was confirmed by accurate mass analysis (Table S1). Ion mobility mass spectrometry (IM–MS) unambiguously established that all investigated CB7-

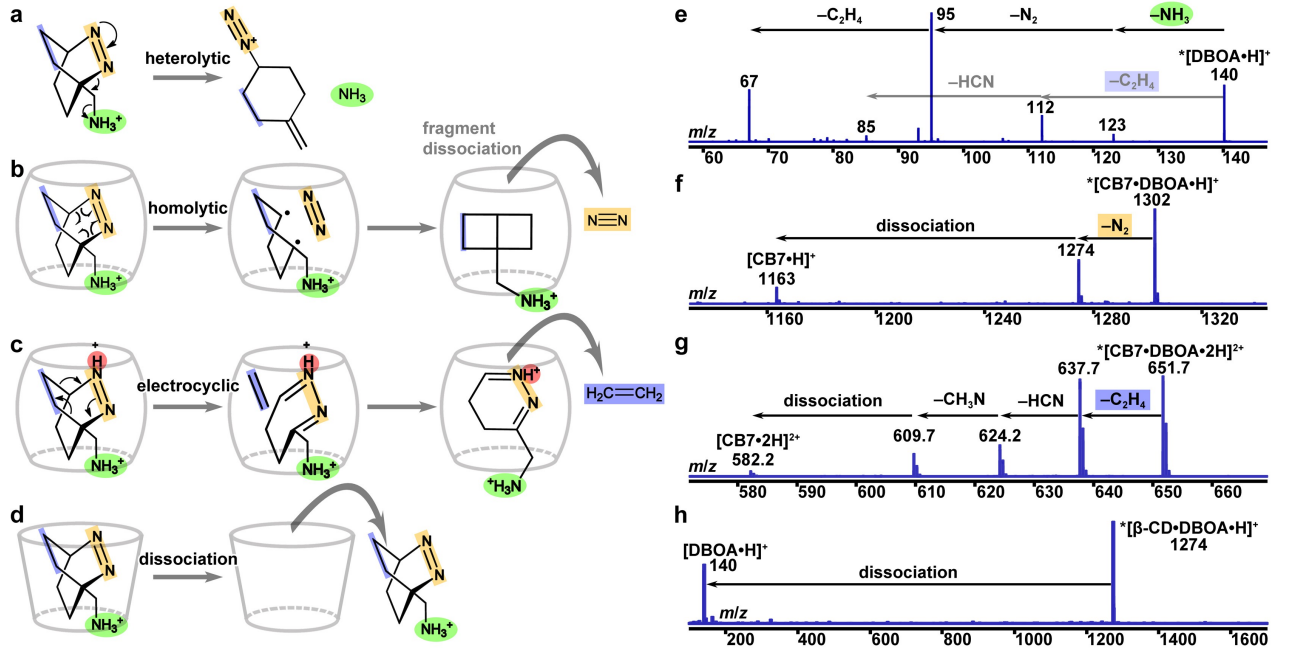

Figure 2. Major reaction pathways of DBOA under CID conditions in the gas phase. a) Free DBOA eliminates NH_3 (green) upon thermal activation as major pathway (heterolytic covalent bond cleavage). b) Inside the cavity of CB7, and with the NH_3-moiety being stabilized by the CB portal, it eliminates N_2 (orange) upon activation (homolytic covalent bond cleavage). c) An additional protonation (red) of the azo group inside CB7 blocks the N_2-elimination pathway, such that DBOA undergoes a retro-Diels–Alder reaction (electrocyclic ring opening) to eliminate C_2H_4 (blue). d) When complexed by β-CD, collision-induced dissociation into the free host and guest takes place (noncovalent bond cleavage). See Supporting Information Sections 3 and 4 for a detailed analysis. Corresponding CID MS/MS spectra of e) $[DBOA{\cdot}H]^+$, f) $[CB7{\cdot}DBOA{\cdot}H]^+$, g) $[CB7{\cdot}DBOA{\cdot}2H]^{2+}$, and h) $[\beta\text{-}CD{\cdot}DBOA{\cdot}H]^+$, where precursor ions are marked with an asterisk.

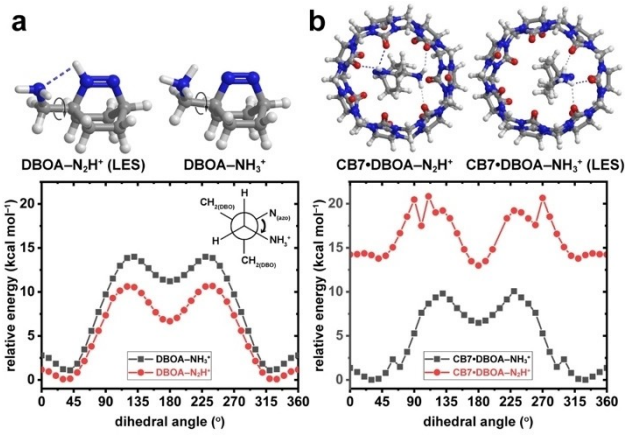

Figure 3. Molecular models of a) $[DBOA{\cdot}H]^+$ and b) $[CB7{\cdot}DBOA{\cdot}H]^+$ for different protonation states, at the azo or amino group with the lowest-energy state (LES) indicated and associated dihedral energy profiles. The dashed lines indicate hydrogen bonds. Curly arrows denote the dihedral angle θ of the rotatable N–C–C–N bond. Note that the encapsulation of DBOA inside CB7 energetically favors protonation of the amino group due to enhanced electrostatic interactions with the CB portal. Note also that the protonation of the azo nitrogen that is distal to the amino group (not shown) results in higher-energy structures.

guest/product complexes were of the inclusion type (Table S2), that is, the observed processes are inner-phase reactions. Additionally, the doubly protonated complex, $[CB7{\cdot}DBOA{\cdot}2H]^{2+}$, can be observed and isolated from the profile mass spectrum. CID experiments showed that the fragmentation of $[CB7{\cdot}DBOA{\cdot}2H]^{2+}$ follows yet another route (Figure 2c,g), exclusively the electrocyclic C_2H_4 elimination pathway. These observations pointed to a fascinating switch-over in chemoselectivity, which we investigated in depth.

The modulation of the gas-phase reactivity of $[DBOA{\cdot}H]^+$ by CB7-encapsulation can be formally explained by classical organic-chemical reaction mechanisms and reactivity-selectivity principles (Figure S15). The preferential elimination of NH_3 from free $[DBOA{\cdot}H]^+$ can be mechanistically rationalized as an intramolecular *anti* elimination reaction (Figure 2a), in which the departure of NH_3 as a leaving group is assisted by a heterolytic ring-opening reaction under formation of a diazonium cation, which subsequently eliminates N_2, as demonstrated by the MS/MS spectra (Figure 2e). Upon encapsulation by CB7, the NH_3-elimination pathway becomes unfavorable because the NH_3 moiety is now noncovalently stabilized by electrostatic interactions with the electron-rich carbonyl portal of CB7 (Figure 2b), that is, it becomes a poorer (more basic) leaving group. In this case, a homolytic elimination of N_2 takes place via a radical mechanism, driven by the high stability of molecular dinitrogen. This observation is consistent with previous experimental and computational studies on the thermal deazatization of neutral DBO derivatives that occurs with significant rates at temperatures between 200–

250 °C.[21,22] The elimination is expected to occur via a stepwise homolytic cleavage involving a 1,4-cyclohexanediyl diradical intermediate, which subsequently forms bicyclo-[2.2.0]hexane upon radical recombination and eventually rearranges to yield 1,5-hexadiene—the more flexible and, thus, entropically favored product under thermally activated conditions (Figure S15b).[23]

Protonation of the azo moiety, in the doubly protonated $[CB7{\cdot}DBOA{\cdot}2H]^{2+}$, effectively blocks the homolytic C–N bond cleavage pathway because a highly unstable $[N_2H]^+$ species (instead of N_2) would be formed. Instead, a third pathway is switched on, the C_2H_4-elimination via a concerted retro-Diels–Alder mechanism (Figure 2c), which had also been observed in our previous study of bridgehead-unsubstituted protonated azoalkanes.[13] This pathway subsequently follows a characteristic reaction cascade involving 6 intermediates (all confirmed by accurate mass analysis) through a 1,3-H shift, a second cycloelimination, and a β-elimination reaction, before ultimately dissociating back to $[CB7{\cdot}2H]^{2+}$ and $[CB7{\cdot}H]^+$ (Figure 2g, Figure S12, Figure S15c). The kinetic stability of the $[CB7{\cdot}fragment{\cdot}2H]^{2+}$ complexes is remarkable. In fact, it constitutes the longest discrete inner-phase reaction cascade in the gas phase reported to date (>5 steps).

Organic-chemical bond cleavage reactions are textbook-wise categorized according to three fundamental reaction types (heterolytic, homolytic, and electrocyclic), and the chemical reactivity of protonated DBOA in the gas phase features all of them. The reaction types govern the way we classically write out chemical reaction mechanisms with electron-pushing arrows (double-barbed, single-barbed, or connected in a circle as in Figure 2) and they govern the way we rationalize chemical reactivity through the types of involved frontier molecular orbitals (σ bonds for heterolytic vs SOMO-SOMO for homolytic vs π HOMO–LUMO for electrocyclic reactions) or the energy gaps ($\Delta\varepsilon$) between the interacting orbitals of the two involved reaction partners or products (large $\Delta\varepsilon$ for heterolytic and small $\Delta\varepsilon$ for electrocyclic reactions).[24]

In detail, the thermal decomposition of $DBOA{\cdot}H^+$ can occur through multiple competitive pathways that involve three distinct reaction types and the cleavage of different sets of covalent σ bonds: (1) heterolytic cleavage of the exocyclic C–NH_3 bond under elimination of NH_3, (2) (stepwise) homolytic bond dissociation of the endocyclic C–N=N bonds under elimination of N_2, and (3) an electrocyclic reaction involving a concerted breakage of the endocyclic C–C bonds with elimination of C_2H_4. The third pathway predominates in the doubly protonated $[CB7{\cdot}DBOA{\cdot}2H]^{2+}$ complex. The first pathway is the predominant pathway for uncomplexed $[DBOA{\cdot}H]^+$, in competition with the third pathway, while the second pathway is exclusive for the $[CB7{\cdot}DBOA{\cdot}H]^+$ complex. As an added layer of mechanistic complexity, the system also features a competition between covalent and noncovalent bond cleavage pathways (Figure 2a–c vs Figure 2d), which has been scrutinized before[13] and is therefore omitted from the chemical reactivity discussion.

In order to rationalize the noncovalent differentiation of the covalent chemoselectivity in detail, we carried out density-functional theoretical (DFT) calculations for the lowest-energy states (LES) and transition states (TS) of the different reaction pathways (Figure 3, 4). We used the wB97XD/6-31G* level of theory, since this dispersion-corrected hybrid functional is known to capture reasonably well intramolecular and supramolecular interactions between non-bonded moieties, such as those within host–guest complexes.[25] In an attempt to obtain a holistic view of the energy surface, which—as we found later—is essential for the understanding of the observed chemoselectivity, we performed calculations around the dihedral angle θ (as depicted in Figure 3) of the bridgehead C–CH_2NH_2 bond; it is the only non-terminal, rotatable bond in the DBOA molecular framework. This dihedral angle θ can serve as a simple measure of the relative positions of the two distinctive functional groups (–NH_3^+ and –N=N–) and scanning around it can effectively sample the chemical reactivity of the competing pathways across the entire conformational space. Note that the energetic reference point of all calculated intermediates at all dihedral arrangements in Figure 4 is the global lowest-energy conformation (near 30°, marked as LES in Figure 3). In the interpretation of the computational data, we focus on relative energetic trends, because the accuracy of the selected method cannot be fully validated. Specifically, the only available experimental benchmarks, the activation enthalpy and entropy for thermal extrusion of N_2 from DBO in the gas phase, $\Delta H^{\ddagger}$ ca. 45 kcal mol^{-1} and $\Delta S^{\ddagger}$ ca. 10 cal K^{-1} mol^{-1},[22] indicates a good agreement with the computed enthalpy for homolytic C–N=N bond cleavage, $\Delta H^{\ddagger} = 47.0$ kcal mol^{-1}, but a larger variation for the computed entropy, $\Delta S^{\ddagger} = 5.4$ cal K^{-1} mol^{-1} (Table S4). Cross-validation of the transition-state energies using higher levels of theory shows excellent consistency (Table S3) which supports the choice of wB97XD/6-31G* as default.

As can be seen from Figure 4, the activation barriers for the three reaction types are dramatically and selectively affected by the supramolecular encapsulation (compare left and right graphs in Figure 4). In particular, the pathways for elimination of NH_3 and C_2H_4 (grey and blue) become energetically disfavored in the $[CB7{\cdot}DBOA{\cdot}H]^+$ complex while the elimination of N_2 is energetically favored (red), especially at elevated temperature. Even though the precise temperature under the CID conditions is unknown, the sensible temperature window between 300–700 K (indicated as dashed lines in Figure 4c,d) nicely explains the experimental results in regard to the competitive heterolytic and electrocyclic pathways for free DBOA and the predominance of the homolytic pathway for the singly protonated CB7 complex.

The computational results in Figure 4 can be semi-quantitatively interpreted in regard to the described structure–activity relationships and organic-chemical reaction mechanisms. As expected, although $[DBOA{\cdot}H]^+$ is most stable when the amino and azo groups are adjacent (Figure 3a), the elimination of NH_3 occurs from the *anti*-coplanar configuration (i.e., $\theta = 180°$, grey graph in Fig-

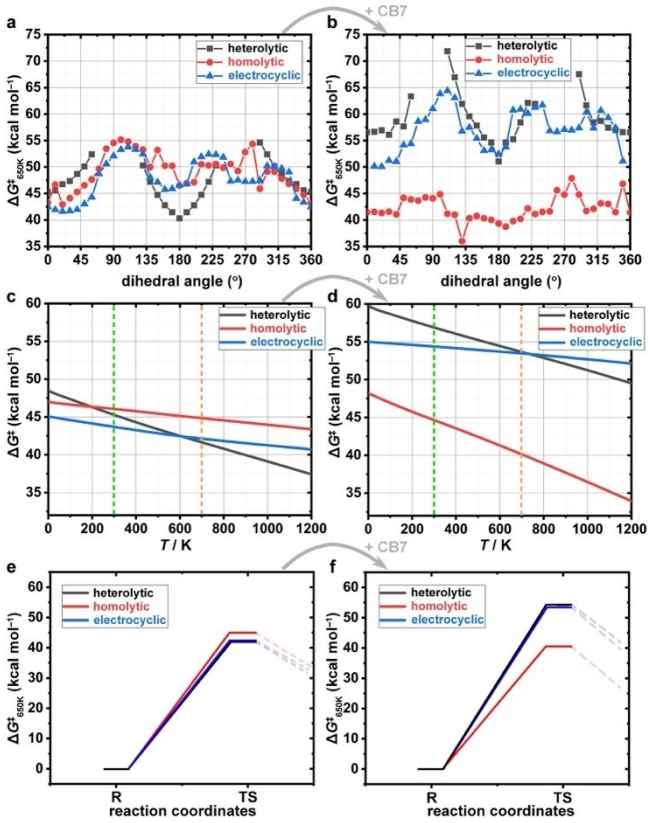

Figure 4. Variation of the Gibbs free energy of activation $\Delta G^{\ddagger}$ of the three reaction pathways for free $[DBOA{\cdot}H]^+$ (left) upon inclusion complexation by CB7 (right). $\Delta G^{\ddagger}$ of a) $[DBOA{\cdot}H]^+$ and b) $[CB7{\cdot}DBOA{\cdot}H]^+$ against dihedral angle at 650 K. For $[DBOA{\cdot}H]^+$, the global minimum of $\Delta G^{\ddagger}$ occurs in the NH_3-elimination pathway at $\theta = 180°$ (dark grey) followed by that of the C_2H_4-elimination at $\theta \approx 30°$ (blue). For $[CB7{\cdot}DBOA{\cdot}H]^+$, N_2-elimination (red) is favorable across all θ values. Boltzmann-weighted values for $\Delta G^{\ddagger}$ of c) $[DBOA{\cdot}H]^+$ and d) $[CB7{\cdot}DBOA{\cdot}H]^+$ of the different dihedral-angle dependent structures against temperature, where the y-intercept represents $\Delta H^{\ddagger}$ and the slope represents $-\Delta S^{\ddagger}$. Room temperature (300 K) is marked as a green dotted line and the onset temperature of thermal decomposition of CB7 (ca. 700 K)[26] is marked as the orange dotted line. In the case of free $[DBOA{\cdot}H]^+$, NH_3-elimination becomes kinetically more favorable above a critical temperature of 600 K due to the larger positive $\Delta S^{\ddagger}$. For $[CB7{\cdot}DBOA{\cdot}H]^+$, N_2-elimination is kinetically favorable across the entire temperature range. See Figure S16 for lowest energy transition state structures (TS). Note that the energetic reference point of all calculated TS at all dihedral arrangements in Figure 4 is the global lowest-energy conformation (LES, θ ca. 30°) in Figure 3. Shown in panels (e) and (f) are the conventional reaction coordinates connecting the reactant R to the (first) transition state TS for the heterolytic (black), homolytic (red), and electrocyclic (blue) cleavages of free $[DBOA{\cdot}H]^+$ and $[CB7{\cdot}DBOA{\cdot}H]^+$ at $T = 650$ K.

ure 4a). Complexation of the NH_3 group by the carbonyl portal of the CB7 deteriorates its leaving group propensity electrostatically which is reflected in a more than 10 kcal mol^{-1} activation energy increase of this pathway, according to DFT calculations (compare grey data points in Figure 4a,b). The extrusion of C_2H_4 in free DBOA occurs from the tautomer with a protonated azo group which activates the retro-Diels–Alder reaction. In contrast to the elimination of NH_3, the electrocyclic reaction (blue entries in Figure 4a,b) takes place from an approximately *cis* coplanar conformation of the NH_2 group with the protonated azo group, where an intramolecular hydrogen-bond contributes (Figure 3a). The calculations predict that this electrocyclic pathway is certainly competitive (Figure 4a) if not preferred (Figure 4c) to the heterolytic pathway for free $[DBOA{\cdot}H]^+$, and it is also found to be at least a minor pathway in the CID experiments (Figure 2e). Equally important, the calculations show that the electrocyclic pathway is also energetically disfavored by more than 10 kcal mol^{-1} in the $[CB7{\cdot}DBOA{\cdot}H]^+$ complex, because the protonated azo group is electrostatically stabilized by the CB7 carbonyl rim; this deactivates the electrocyclic reaction relative to that of uncomplexed $[DBOA{\cdot}H]^+$ because the dienophilic fragment becomes less electron-deficient.

From a catalytic point of view, the computational results show that the homolytic reaction pathway (red data points in Figure 4a,b), which is the energetically least favorable and experimentally elusive one for uncomplexed $[DBOA{\cdot}H]^+$, becomes favorable in relative and absolute terms in the $[CB7{\cdot}DBOA{\cdot}H]^+$ complex. In relative terms, because the other two competitive reaction types are strongly disfavored in the noncovalent assembly, and in absolute terms because the reaction has a positive volume of activation, and the packing coefficient of the corresponding transition state (52 %) is more favorable since closer to the ideal value (55 %) than the packing in the loose substrate complex (48 %). Packing coefficient arguments, which empirically reflect a balance of enthalpic and entropic effects in host–guest complexes, have been previously used to account for the favorable elimination of C_2H_4 from the parent $[DBO{\cdot}H]^+$,[13] and the same arguments will obviously apply for the elimination of any other molecular fragment as well, N_2 in the case of the homolytic bond cleavage of $[DBOA{\cdot}H]^+$. Notably, based on the DFT calculations, the lowering of $\Delta G^{\ddagger}$ upon CB-encapsulation is due to the large and more positive $\Delta S^{\ddagger}$ value rather than a more negative $\Delta H^{\ddagger}$ (See Supporting Information Section 5.5 for further discussion on the assumptions). The latter does not change significantly inside the cavity of CB7 (47.0 kcal mol^{-1} for $[DBOA{\cdot}H]^+$ and 48.2 kcal mol^{-1} for $[CB7{\cdot}DBOA{\cdot}H]^+$, data points at $T = 0$ K in Figure 4c,d), while the former can be deduced from the different slopes of the red graphs in Figure 4c,d. We speculate that this entropic effect is due to the decreased steepness of the potential well,[27] where weakening of the C–N bonds is counterbalanced by the enhanced dispersion interactions with the cavity wall of CB7 as the bond elongates. In the relevant temperature range between 300–700 K, the absolute stabilization due to this effect accounts for 2–4 kcal mol^{-1}, which falls in the typical range of stabilization of the transition state for a fragmentation reaction due to increased dispersion interactions.[13,28,29]

Moreover, there appears to be an additional entropic effect that favors the homolytic pathway in the CB7 cavity, because the dihedral angle dependence for deazetization largely disappears when complexed inside CB7 (red data points in Figure 4b), while in the uncomplexed form a preferential cleavage near the *cis* conformation was ob-

served (Figure 4a). In the latter, the ammonium group is stabilized by the neighboring azo group (Figure 3, grey data points), which leads to a favorable homolytic cleavage from this conformation (ground-state effect), while in the former, the ammonium group is immersed in electrostatic interactions with the carbonyl corona of CB7, which essentially allows for a free rotation of the bicyclic residue and a homolytic reaction essentially from any dihedral angle. It should be noted that the entropic component of this (restricted) free rotor effect is only partially included in the Boltzmann-weighted free energies for the homolytic bond dissociation, and that it is estimated to favor the reaction pathway by an additional 1–2 kcal mol^{-1} according to related approximations for supramolecular complexes.[30–32]

Note that the protonation of the azo group in the CB7 complex, which requires a double protonation to form $[CB7{\cdot}DBOA{\cdot}2H]^{2+}$, results experimentally in an exclusive retro-Diels–Alder reaction, that is, the electrocyclic pathway as the third covalent reaction pathway is "switched on" (Figure 2c,g). Calculations further rationalize that the second protonation, that of the azo group, takes place at the distal azo nitrogen, the one more remote from the already protonated ammonium group (Figure S21). This geometry is not only expected on account of intramolecular charge repulsion, but also on account of the complementary stabilization that the protonation of the distal azo nitrogen can receive by electrostatic interactions with the second carbonyl portal of CB7, the one that is not involved in already stabilizing the ammonium group. This "bi-dentate" stabilization of $[CB7{\cdot}DBOA{\cdot}2H]^{2+}$ is unique for the noncovalent assembly, which accounts also for the failure to observe the *uncomplexed* doubly charged $[DBOA{\cdot}2H]^{2+}$ species experimentally, by mass spectrometry. Consequently, the peculiar electrocyclic reactivity of the $[CB7{\cdot}DBOA{\cdot}2H]^{2+}$ complex is also the genuine result of a noncovalent reaction control, allowing an otherwise disfavored double protonation.

It should also be noted that the electrocyclic reaction is the only sensible and computationally verified (Figure S22) covalent pathway for $[CB7{\cdot}DBOA{\cdot}2H]^{2+}$ because homolytic N_2 elimination cannot occur due to the azo group protonation, while the heterolytic pathway (which could be computationally described for the singly charged $[CB7{\cdot}DBOA{\cdot}H]^{+}$) is disfavored, because the mechanistically important conjugatively electron-donating effect by the distal azo nitrogen (Figure 2a, Figure S15) is blocked by protonation.

Conclusion

Macrocyclic encapsulation of guest molecules is well known to activate or switch their chemical reactivity in solution.[3,33–37] However, in the gas phase, when thermally activated, host–guest complexes generally undergo noncovalent bond dissociations. Constrictive binding in host–guest complexes can exceptionally activate covalent bond dissociation as a competitive reaction pathway. We have now established, by employing a functionalized azoalkane as guest, that noncovalent interactions can be deliberately used to modulate covalent reactions such that the full spectrum of organic-chemical reaction types can be covered, ranging from heterolytic bond cleavage (dominant for the uncomplexed monoprotonated guest) to homolytic bond cleavage (exclusive for the protonated host–guest complex) to a concerted cyclo-reversion reaction (specific for the doubly protonated host–guest complex). These gas-phase results, which can be comprehensively computationally and mechanistically rationalized, can be viewed as an example of "mode-selective supramolecular chemistry". They show how a noncovalent approach can be employed to gain control over chemoselectivity and how to steer multiple pathways of thermally activated reactions of small molecules. These results are expected to inspire our vision of how encapsulating supramolecular catalysts can be used regardless of the surrounding phase of matter, and how a differential stabilization of transition states inside host molecules, the arrangement of functional groups in confined environments, the targeted occupation of charges, and constrictive binding in nano-space can be used in the rational design of functional synthetic materials as well as the understanding of enzymatically active proteins.

Acknowledgements

S.M., N.M., E.K., and T.C.L. are grateful to the Research Project Grant (RPG-2016-393) funded by the Leverhulme Trust. H.L. and T.C.L. are grateful to the Studentship funded by the A*STAR-UCL Research Attachment Programme through the EPSRC M3S CDT (EP/L015862/1). The authors acknowledge the use of the UCL Myriad High Performance Computing Facility (Myriad@UCL), and associated support services, in the completion of this work. The authors are grateful to the UK Materials and Molecular Modelling Hub for computational resources, which are partially funded by EPSRC (Grant EP/P020194/1). WMN thanks the DFG for grant NA-686/8 within the priority program SPP 1807 "Control of London Dispersion Interactions in Molecular Chemistry". EK acknowledges the University of Jyväskylä for access to instrumentation. Open Access funding enabled and organized by Projekt DEAL.

Conflict of Interest

The authors declare no conflict of interest.

Data Availability Statement

The data that support the findings of this study are available from the corresponding author upon reasonable request.

Keywords: Cucurbiturils · Gas-Phase Chemistry · Host–Guest Complexes · Mass Spectrometry · Reactivity Modulation

[1] H. Zhao, S. Sen, T. Udayabhaskararao, M. Sawczyk, K. Kučanda, D. Manna, P. K. Kundu, J.-W. Lee, P. Král, R. Klajn, *Nat. Nanotechnol.* **2016**, *11*, 82–88.
[2] J. Kang, J. Rebek, *Nature* **1997**, *385*, 50–52.
[3] T. S. Koblenz, J. Wassenaar, J. N. H. Reek, *Chem. Soc. Rev.* **2008**, *37*, 247–262.
[4] S. Ege, *Organic Chemistry: structure and reactivity*, Houghton Mifflin Co., Boston, **2004**.
[5] M. J. Bronikowski, W. R. Simpson, R. N. Zare, *J. Phys. Chem.* **1993**, *97*, 2204–2208.
[6] R. N. Zare, *Science* **1998**, *279*, 1875–1879.
[7] A. Thomas, L. Lethuillier-Karl, K. Nagarajan, R. M. A. Vergauwe, J. George, T. Chervy, A. Shalabney, E. Devaux, C. Genet, J. Moran, *Science* **2019**, *363*, 615–619.
[8] E. Kalenius, D. Moiani, E. Dalcanale, P. Vainiotalo, *Chem. Commun.* **2007**, 3865–3867.
[9] H. Zhang, E. S. Paulsen, K. A. Walker, K. E. Krakowiak, D. V. Dearden, *J. Am. Chem. Soc.* **2003**, *125*, 9284–9285.
[10] L. M. Nuwaysir, J. A. Castoro, C. L. C. Yang, C. L. Wilkins, *J. Am. Chem. Soc.* **1992**, *114*, 5748–5751.
[11] C. A. Schalley, C. Verhaelen, F. G. Klärner, U. Hahn, F. Vögtle, *Angew. Chem. Int. Ed.* **2005**, *44*, 477–480.
[12] S. W. Heo, T. S. Choi, K. M. Park, Y. H. Ko, S. B. Kim, K. Kim, H. I. Kim, *Anal. Chem.* **2011**, *83*, 7916–7923.
[13] T.-C. Lee, E. Kalenius, A. I. Lazar, K. I. Assaf, N. Kuhnert, C. H. Grün, J. Jänis, O. A. Scherman, W. M. Nau, *Nat. Chem.* **2013**, *5*, 376–382.
[14] X. Zhang, G. Gramlich, X. Wang, W. M. Nau, *J. Am. Chem. Soc.* **2002**, *124*, 254–263.
[15] M. A. Alnajjar, W. M. Nau, A. Hennig, *Org. Biomol. Chem.* **2021**, *19*, 8521–8529.
[16] M. B. More, D. Ray, P. B. Armentrout, *J. Am. Chem. Soc.* **1999**, *121*, 417–423.
[17] D. V. Dearden, T. A. Ferrell, M. C. Asplund, L. W. Zilch, R. R. Julian, M. F. Jarrold, *J. Phys. Chem. A* **2009**, *113*, 989–997.
[18] F. Yang, D. V. Dearden, *Isr. J. Chem.* **2011**, *51*, 551–558.
[19] H. Zhang, T. A. Ferrell, M. C. Asplund, D. V. Dearden, *Int. J. Mass Spectrom.* **2007**, *265*, 187–196.
[20] W. Adam, M. A. Miranda, *J. Org. Chem.* **1987**, *52*, 5498–5500.
[21] M. B. Reyes, B. K. Carpenter, *J. Am. Chem. Soc.* **2000**, *122*, 10163–10176.
[22] K. S. Khuong, K. N. Houk, *J. Am. Chem. Soc.* **2003**, *125*, 14867–14883.
[23] S. G. Cohen, R. Zand, *J. Am. Chem. Soc.* **1962**, *84*, 586–591.
[24] I. Fleming, *Molecular orbitals and organic chemical reactions*, Wiley, Hoboken, **2011**.
[25] N. Mardirossian, M. Head-Gordon, *Mol. Phys.* **2017**, *115*, 2315–2372.
[26] J. Lagona, P. Mukhopadhyay, S. Chakrabarti, L. Isaacs, *Angew. Chem. Int. Ed.* **2005**, *44*, 4844–4870.
[27] H.-X. Zhou, M. K. Gilson, *Chem. Rev.* **2009**, *109*, 4092–4107.
[28] R. Warmuth, J. L. Kerdelhué, S. Sánchez Carrera, K. J. Langenwalter, N. Brown, *Angew. Chem. Int. Ed.* **2002**, *41*, 96–99.
[29] S. Sánchez Carrera, J. L. Kerdelhué, K. J. Langenwalter, N. Brown, R. Warmuth, *Eur. J. Org. Chem.* **2005**, 2239–2249..
[30] M. Mammen, E. I. Shakhnovich, G. M. Whitesides, *J. Org. Chem.* **1998**, *63*, 3168–3175.
[31] H. J. Schneider, *Angew. Chem. Int. Ed.* **2009**, *48*, 3924–3977.
[32] S. Grimme, *Chem. Eur. J.* **2012**, *18*, 9955–9964.
[33] M. Yoshizawa, M. Tamura, M. Fujita, *Science* **2006**, *312*, 251–255.
[34] A. L. Koner, C. Márquez, M. H. Dickman, W. M. Nau, *Angew. Chem. Int. Ed.* **2011**, *50*, 545–548.
[35] V. Martí-Centelles, A. L. Lawrence, P. J. Lusby, *J. Am. Chem. Soc.* **2018**, *140*, 2862–2868.
[36] Q. Zhang, L. Catti, K. Tiefenbacher, *Acc. Chem. Res.* **2018**, *51*, 2107–2114.
[37] G. Olivo, G. Capocasa, D. Del Giudice, O. Lanzalunga, S. Di Stefano, *Chem. Soc. Rev.* **2021**, *50*, 7681–7724.

Manuscript received: March 8, 2023
Accepted manuscript online: May 10, 2023
Version of record online: May 31, 2023